Structural phases of strained $LaAlO_3$ driven by octahedral tilt instabilities

Alison J. Hatt[1] and Nicola A. Spaldin[1,2]
[1]*Materials Department, University of California, Santa Barbara, California 93106, USA*
[2]*Department of Materials, ETH Zurich, Wolfgang-Pauli-Strasse 10, CH-8093 Zurich, Switzerland*
(Received 4 October 2010; published 1 November 2010)

We investigate the effect of epitaxial strain on [001]-oriented $LaAlO_3$ using first-principles density-functional calculations. We find a series of structural phase transitions between states characterized by different patterns of tilting of the AlO_6 octahedra. By tuning the biaxial strain from compressive to tensile, we induce an evolution in the crystal structure in which the tilt axis changes from out of plane to in plane, corresponding to space groups $I4/mcm$ and $Imma$. We also study the effect of uniaxial relaxation of the usual biaxial epitaxial constraint and explore this as a mechanism for selectively stabilizing different patterns of octahedral tilts.

DOI: 10.1103/PhysRevB.82.195402 PACS number(s): 68.60.Bs, 61.50.Ks, 77.55.Px, 81.05.Zx

I. INTRODUCTION

Oxides in the ABO_3 perovskite family present a multitude of functional properties and are widely renowned for their potential in technological applications. Construction of heteroepitaxial thin films is being actively explored as a route to further enhance and expand on the existing oxide functionalities. The presence of an interface between an oxide and a substrate can dramatically affect material properties, particularly if a film is grown coherently so that its in-plane lattice constant is forced to match that of the substrate. The resulting heteroepitaxial strain has been credited, for example, with dramatically enhancing the ferroelectric polarization and Curie temperature in thin-film $BaTiO_3$ (Ref. 1) and inducing ferroelectricity in usually nonpolar $SrTiO_3$.[2] In addition to ferroelectric distortions, we increasingly find repercussions of strain in the patterns of rigid rotations of the corner-sharing BO_6 octahedral units. These changes in rotation have been invoked to account for such phenomena as the strain dependence of magnetic properties, as a result of the corresponding changes in the electronic bandwidth.[3,4] In this work, we use density-functional theory to examine the effect of epitaxial strain on the rotational instabilities in $LaAlO_3$ (LAO). LAO is an ideal model system in which to isolate the interplay between strain and rotations because it exhibits only rotational distortions in its ground state with no indications of ferroelectric or Jahn-Teller instabilities.

We are also motivated by a need to understand the influence of octahedral rotations in oxide heterostructures such as $LAO/SrTiO_3$ (STO), which has been reported to form a highly conductive electron gas at the interface in spite of the insulating nature of the two parent compounds.[5] The propagation of octahedral rotations across the interface is likely to be relevant to its electronic properties, but microscopic techniques have limited access to the positions of oxygen ions.[6] An improved understanding of the effect of strain on the parent compound LAO is therefore highly desirable.

Here we investigate the effect of biaxial strain in LAO. We find that the bulk $R\bar{3}c$ structure is destabilized by the constraint of coherent epitaxy and that compressive and tensile biaxial strains greater than $\pm 0.2\%$ stabilize previously unidentified phases of LAO. In addition, we find that uniaxial relaxation of the biaxial epitaxial constraint stabilizes a third phase. The primary structural differences between these strain-stabilized phases and the parent phase are the patterns of octahedral rotations, and our analysis of the transition between them provides insight into the coupling between strain and rotations in LAO and similar ABO_3 perovskites.

II. CALCULATION DETAILS AND NOTATION

For all calculations we use the local-density approximation (LDA) of density-functional theory as implemented in the Vienna *ab initio* simulation package, VASP.[7] We use the projector augmented wave method[8,9] with the default VASP LDA potentials (La, Al, and O) and a plane-wave energy cutoff of 800 eV. We use a ten-atom rhombohedral unit cell with a $5\times5\times5$ k-point sampling. To determine ground-state structures we relax ionic positions to a force tolerance of 1 meV/Å. Space-group determinations are performed with the FINDSYM symmetry analysis software.[10]

Strain is calculated as $(a-a_0)/a_0$, where a_0 is the LDA equilibrium lattice parameter. We use the notation a,b,c to denote the pseudocubic (pc) lattice constants (except where noted), which correspond to the crystallographic directions $[100]_{pc}$, $[010]_{pc}$, and $[001]_{pc}$. Our computational unit cell,

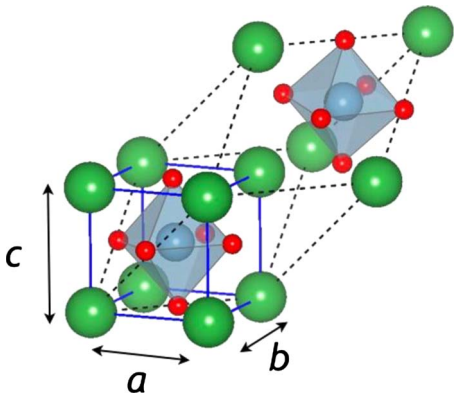

FIG. 1. (Color online) Relationship between computational unit cell (dashed line) and pseudocubic lattice parameters a,b,c (solid blue line). La atoms shown in green (dark gray); Al atoms shown in blue (light gray) at center of oxygen octahedra.

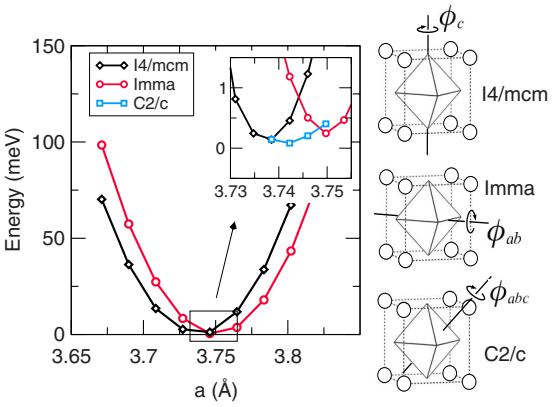

FIG. 2. (Color online) Energy per five-atom formula unit of LAO as a function of in-plane lattice constant a (constant volume). Energy is given relative to unconstrained $R\bar{3}c$. Right: schematics of pseudocubic unit cells showing axes of octahedral rotations in the three phases.

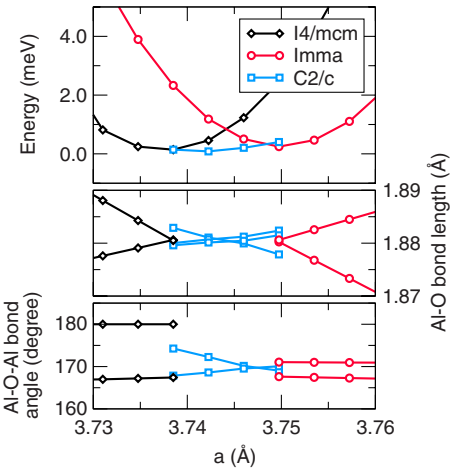

FIG. 3. (Color online) Transition details as a function of in-plane lattice constant a (constant volume). Top panel: energy per five-atom formula unit; middle panel: Al-O bond distances; and lower panel: Al-O-Al bond angles.

shown in Fig. 1, is defined by lattice vectors $(0,b,c)$, $(a,0,c)$, and $(a,b,0)$. Lattice distortions comprised of rigid octahedral rotations are described by the angles of rotation around the pseudocubic axes, ϕ_a, ϕ_b, and ϕ_c, as shown in Fig. 2. For completeness we also give the Glazer notations for our structures, where, e.g., ϕ_a is written as $a^+b^0c^0$ if consecutive octahedra along a rotate in the same direction (in phase) or $a^-b^0c^0$ if consecutive octahedra rotate in the opposite directions (out of phase).[11] Multiple subscripts indicate a compound rotation, e.g., ϕ_{ab} denotes rotation around the ab axis (crystallographic direction $[110]_{pc}$). (Note that the ϕ_i are not strictly independent, however, a rigorous decomposition made using irreducible representations yields nearly identical results.)

III. BIAXIAL STRAIN

The bulk crystal structure of LAO deviates from the ideal $Pm\bar{3}m$ perovskite by out-of-phase rotations around the crystallographic [111] axis (ϕ_{abc}, Glazer system $a^-a^-a^-$) that lower the symmetry to space group $R\bar{3}c$, and an accompanying rhombohedral distortion. We reproduce this structure by relaxing lattice parameters and atom positions in our ten-atom unit cell and calculate a rhombohedral angle of 60.2° and an equilibrium lattice constant of 5.298 Å (pseudocubic a_0=3.746 Å), which underestimates the experimentally determined value by ~1%, a common artifact of LDA calculations. We calculate ϕ_{abc}=5.98°, close to the experimentally determined value.[12]

To mimic clamping to a substrate, we enforce a square lattice in the plane of epitaxy (a=b) and constrain the value of in-plane lattice parameter a while relaxing the out-of-plane parameter c and atom positions. We also allow a $[110]_{pc}$ shear of the unit cell. The resulting structure, for a=3.746 Å has space group $C2/c$; it retains the ϕ_{abc} rotations of the bulk and has a relaxed monoclinic angle β=90.3°. We then investigate the effect of biaxial strain by adjusting the value of a. For strains of −2 to +2 % we identify two competing phases with space groups $I4/mcm$ and $Imma$. The resulting energy-versus-strain phase diagram is shown in Fig. 2 and details of the transition region are shown in Fig. 3. To facilitate fine sampling near the transition we do not relax c in these calculations but instead maintain the equilibrium volume. Later we relax this constraint and find no qualitative changes to the phase diagram. We find that the shear distortion is only energy lowering for the $C2/c$ phase and all other phases retain β=90°.

At very small strains of −0.2 to 0.1 %, the ground state is $C2/c$. The structure exhibits the ϕ_{abc} rotations of the bulk and has a relaxed monoclinic angle β=90.3°. As strain is increased, the $C2/c$ phase becomes rapidly unstable and the system transitions to $Imma$ or $I4/mcm$, depending on the sign of the strain. Compressive strain greater than −0.2% stabilizes the $I4/mcm$ phase, in which the lattice distortion consists of ϕ_c rotations (Glazer system $a^0a^0c^-$) whereas tensile strain greater than 0.1% stabilizes the $Imma$ phase, com-

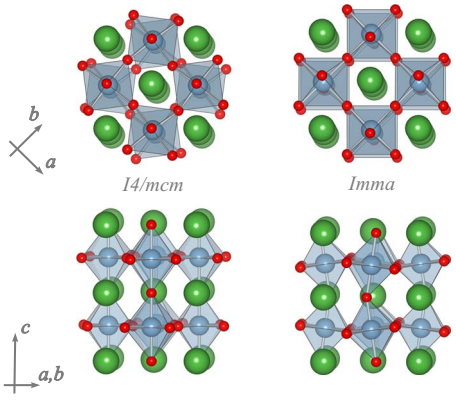

FIG. 4. (Color online) Crystal structures of $I4/mcm$ (left) and $Imma$ (right) phases, the ground states for compressive- and tensile-strained LAO, respectively. Upper figures depict $[001]_{pc}$ projection (ab plane); lower figures depict $[110]_{pc}$ projection. La atoms shown in green (dark gray); Al atoms shown in blue (light gray) at center of oxygen octahedra.

TABLE I. Summary of the rotational modes and resulting space groups found in LAO under various strain states.

	Rotation angles		Rotation axis	Glazer notation	Conditions for stability
$R\bar{3}c$	$\phi_a=\phi_b=\phi_c\neq 0$		$[111]$	$a^-a^-a^-$	Unconstrained
$C2/c$	$\phi_a=\phi_b\neq 0$	$\phi_c\neq 0$	$[111]_{pc}$	$a^-a^-c^-$	$-0.2\%<\eta<0.1\%$, biaxial
$I4/mcm$	$\phi_a=\phi_b=0$	$\phi_c\neq 0$	$[001]_{pc}$	$a^0a^0c^-$	$\eta<-0.2\%$, biaxial
$Imma$	$\phi_a=\phi_b\neq 0$	$\phi_c=0$	$[110]_{pc}$	$a^-a^-c^0$	$\eta>0.1\%$, biaxial
$Fmmm$	$\phi_a\neq 0$	$\phi_b=\phi_c=0$	$[100]_{pc}$	$a^-b^0c^0$	Small uniaxial strain, $a>b$

prised of ϕ_{ab} rotations ($a^-a^-c^0$), as shown in Fig. 4. Thus, the bulklike $C2/c$ phase is found only in a very narrow range of strain near the equilibrium lattice parameter. These results are summarized in Table I and structural parameters for each phase at a representative strain are given in Table II. (Note that the precise range of stability for the three ground-state phases is difficult to identify from total energies. Thus we obtain our predicted range of the $C2/c$ phase by calculating the zone-center phonons of each phase as a function of strain and comparing the frequencies of the softest nontrivial modes.)

To examine the coupling between strain and rotations, we decompose the distortion from a high-symmetry parent phase with space group $P4/mmm$ in terms of irreducible representations (or irreps) using the software ISODISPLACE.[13] We find that the dominant irreps are A_4^- and A_5^-, which correspond to ϕ_c and ϕ_{ab} rotations, respectively. The evolution of the irrep amplitudes in the lowest-energy structures is shown in Fig. 5. We also calculate ϕ_c and ϕ_{ab} from the angles between neighboring octahedra (in the manner of Ref. 14) to provide an approximate correspondence between irrep amplitude and rotation angle (Fig. 5). Within $I4/mcm$ and $Imma$ we find a roughly linear dependence of rotation angles on lattice parameter.

Our results suggest a simple model to describe the response of LAO to biaxial strain. In bulk LAO the ϕ_{abc} rotations reduce the bonding distances around the small La cation and minimize the sum of Coulombic and repulsive energies, while the dimensions of the octahedra are determined by the strongly covalent Al-O bonds.[15] Within this lattice, strain-related changes in lattice spacing are accommodated by changes in either the rotations or the Al-O bond lengths. Under biaxial strain, we find two distinct responses within the range of strains investigated, as seen in the evolution of Al-O distances and octahedral rotations, shown in Fig. 3. At very small values of strain (−0.2 to 0.1 %) the changes in lattice dimensions are accommodated primarily by rotations while Al-O distances remain nearly constant, and the system remains in the $C2/c$ phase. Under compressive (tensile) strain, transformation to $I4/mcm$ ($Imma$) oc-

TABLE II. Calculated structural parameters of each phase given for a representative value of strain. Note that here the labels a,b,c do not refer to the pseudocubic lattice parameters but to the conventional parameters of the given space group.

	a (Å)	b (Å)	c (Å)	β (deg)	Wyckoff pos.	x	y	z
$C2/c$ (0% strain)	9.15	5.2976	5.2976	54.927	La (4e)	0.0	0.2500	0.25
					Al (4d)	0.25	0.25	0.5
					O (8f)	−0.2652	0.4829	0.2823
					O (4e)	0.0	−0.2804	0.25
$I4/mcm$ (−0.5% strain)	5.2712	5.2712	7.5634		La (4b)	0.0	0.5	0.25
					Al (4c)	0.0	0.0	0.0
					O (8h)	−0.2212	0.2788	0.0
					O (4a)	0.0	0.0	0.25
$Imma$ (0.5% strain)	7.4642	5.3156	5.3156		La (4e)	0.0	0.25	−0.2491
					Al (4c)	0.25	0.25	0.25
					O (8f)	−0.2298	0.0	0.0
					O (4e)	0.0	0.25	0.2894
$Fmmm$ (~0% strain)	7.4800	7.4502	7.5099		La (8i)	0.0	0.0	−0.2501
					Al (8e)	0.25	0.25	0.0
					O (8f)	0.25	0.25	0.25
					O (8g)	−0.2770	0.0	0.0
					O (8h)	0.0	0.2231	0.0

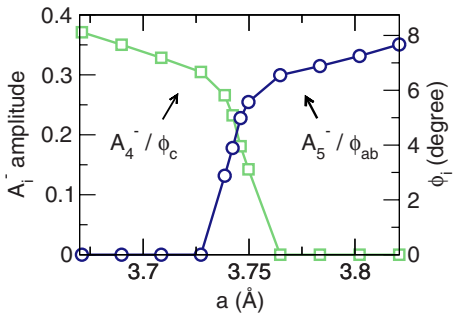

FIG. 5. (Color online) Rotation modes A_i^- and equivalent tilt angles ϕ_j of LAO as a function of in-plane lattice parameter a (constant volume).

curs when ϕ_{ab} (ϕ_c) goes to zero. Increased strain is then accommodated by changes to Al-O distances, while the rotations remain nearly constant. We note that the precise values of strain at which the phase transformations are predicted to occur are dependent on very small energy differences and are therefore somewhat sensitive to the computational parameters used. For example, test calculations performed using the generalized gradient approximation for the exchange-correlation energy indicated small variations in the quantitative details of the phase diagram but the qualitative model does not change significantly.

Similar strain-induced variations in tilt patterns have recently been reported in a number of other perovskite oxides, including $SrRuO_3$,[14] $BiFeO_3$,[16] and $LaNiO_3$.[17] The behavior of LAO is distinct from these systems, however, in the extremely narrow window in which the parent phase is stable and the dramatically different structures stabilized by compressive and tensile strain.

IV. UNIAXIAL RELAXATION OF STRAIN

We next examine the effect of a uniaxial relaxation of tensile strain in LAO. We compare the energetics of ϕ_{ab} rotations (*Imma* phase) to a phase with only ϕ_a rotations (space group *Fmmm*). Under biaxial strain, the *Fmmm* phase is ~0.5 meV higher in energy than *Imma* in the range of strains investigated, but a uniaxial relaxation of the strain, such that $a \neq b$, alters the balance of energy between the two. Starting with atom configurations from the relaxed structures for $a=b$, we vary the ratio a/b and calculate the total energy for the two phases. We maintain a constant in-plane area ab[18] and do not relax c. We first explore the system with $ab=(3.746\ \text{Å})^2$ and find that a 0.5% distortion of a/b stabilizes ϕ_a rotations relative to ϕ_{ab} by ~1 meV. We compare this to the system with $ab=(3.85\ \text{Å})^2$, ~3% tensile strain, and find that the uniaxial relaxation is no longer energetically favorable, and the ground state retains ϕ_{ab} rotations and $a=b$.

Our results indicate that LAO films on substrates with a lattice mismatch of ~0.5% may, in theory, lower their energy through a partial relaxation such that $a \neq b$. The resulting structure exhibits ϕ_a rotations (for $a>b$) in the space group *Fmmm*. In practice, no common growth substrate provides these conditions, but the result is likely to be a general phenomenon in similar materials. The data suggest an explanation for the experimental observation of $a \neq b$ in some coherent films grown on square substrates. For example, $BiFeO_3$ films thinner than 50 nm grown on LAO substrates are reported to have $a \sim 3.84$ Å and $b \sim 3.76$ Å, compared to the substrate parameters $a=b=3.79$ Å, indicating a uniaxial relaxation of the epitaxial constraint.[19] Our results for LAO at 3% tensile strain, which do not predict a uniaxial strain relaxation, are consistent with experimental data for films of LAO on STO (a mismatch strain of 3%). Such films are reported to have square in-plane lattice parameters within an accuracy of 0.01 Å, indicating that any distortion of a/b must be smaller than 0.5%.[20–22]

V. DISABLED OCTAHEDRAL ROTATIONS

Finally, we address the effect of manually disabling octahedral rotations. For this we treat a five-atom tetragonal unit cell in which rotation of the oxygen octahedra is forbidden by symmetry. At each value of epitaxial strain we relax the positions of the ions and calculate the electric polarization using the Berry phase method.[23,24] We find that, while the unstrained system is nonpolar, an abrupt transition to a state with large polarization occurs at −3% strain. The polarization is out of plane and results from a structural distortion within $P4/mmm$ symmetry in which Al and La displace along [001]. A compressive strain of 4% results in a polarization of 38 $\mu\text{C cm}^{-2}$ relative to a centrosymmetric reference structure. These results indicate the existence of an incipient ferroelectric mode that is usually suppressed by the dominant antiferrodistortive rotational modes.

VI. SUMMARY AND DISCUSSION

In summary, we find that several different phases of LAO, characterized by distinct patterns of octahedral rotations, can be stabilized by varying the epitaxial constraints over a range that is readily accessible experimentally. This remarkable structural softness indicates that it is unlikely that the bulk-type ϕ_{abc} rotations will be observed in heteroepitaxial thin films of LAO on any substrate. This has important implications for the interpretation of structural data for LAO films, with particular relevance to investigations of the properties of LAO/STO interfaces.

We find that biaxial strain of −0.2 to 0.1 % results in large changes in octahedral tilt angles in the bulklike $C2/c$ phase of LAO. Larger strains, however, induce a tilt-driven transition to one of three phases in which at least one tilt component is zero ($I4/mcm$, *Imma*, or *Fmmm*). Within these strained phases, we find that changes in lattice parameters related to epitaxial strain are largely accommodated by changes in the Al-O bond lengths, with only small changes to tilt angles and without any significant effect on electronic properties. These findings provide insight to the growing list of complex oxide perovskites in which the rotational distortions are observed to depend on lattice parameters. Given the coupling between rotations and strain in LAO, and its nonpolar structure, we propose it as a model system for explor-

ing new nonlinear optical techniques for probing octahedral rotations.[25]

Finally, for small values of tensile strain we find that a uniaxial relaxation of the strain, such that $a > b$, stabilizes ϕ_a rotations over ϕ_{ab}. Our results suggest a route to selectively stabilize different tilt patterns via the substrate geometry. Conversely, these results also suggest an explanation for the unequal in-plane lattice parameters observed in some epitaxial thin films of perovskites, in which similar energetics of ϕ_a and ϕ_{ab} rotations may drive a distortion of a/b.

ACKNOWLEDGMENTS

This work was supported by the National Science Foundation (NSF), Grants No. NIRT-0609377 (N.A.S.) and No. DMR-0820404 (A.J.H.). Computational support was provided by the MRL Central Facilities under the NSF MRSEC Program, Award No. DMR05-20415, and the CNSI Computer Facilities at UC Santa Barbara, NSF under Grant No. CHE-0321368. We thank J. M. Rondinelli and M. Stengel for helpful discussions.

[1] K. J. Choi *et al.*, Science **306**, 1005 (2004).
[2] J. H. Haeni *et al.*, Nature (London) **430**, 758 (2004).
[3] H. Ishida and A. Liebsch, Phys. Rev. B **77**, 115350 (2008).
[4] D. Fuchs, E. Arac, C. Pinta, S. Schuppler, R. Schneider, and H. v. Löhneysen, Phys. Rev. B **77**, 014434 (2008).
[5] A. Ohtomo and H. Y. Hwang, Nature (London) **427**, 423 (2004).
[6] C. L. Jia, S. B. Mi, M. Faley, U. Poppe, J. Schubert, and K. Urban, Phys. Rev. B **79**, 081405 (2009).
[7] G. Kresse and J. Furthmüller, Phys. Rev. B **54**, 11169 (1996).
[8] P. E. Blöchl, Phys. Rev. B **50**, 17953 (1994).
[9] G. Kresse and D. Joubert, Phys. Rev. B **59**, 1758 (1999).
[10] H. T. Stokes and D. M. Hatch, FINDSYM, 2004, stokes.byu.edu/isotropy.html
[11] A. M. Glazer, Acta Crystallogr., Sect. B: Struct. Crystallogr. Cryst. Chem. **28**, 3384 (1972).
[12] K. A. Müller, W. Berlinger, and F. Waldner, Phys. Rev. Lett. **21**, 814 (1968).
[13] B. Campbell, H. Stokes, D. Tanner, and D. Hatch, J. Appl. Crystallogr. **39**, 607 (2006).
[14] A. T. Zayak, X. Huang, J. B. Neaton, and K. M. Rabe, Phys. Rev. B **74**, 094104 (2006).
[15] P. M. Woodward, Acta Crystallogr., Sect. B: Struct. Sci. **53**, 44 (1997).
[16] A. J. Hatt, N. A. Spaldin, and C. Ederer, Phys. Rev. B **81**, 054109 (2010).
[17] S. May, J. Kim, J. Rondinelli, E. Karapetrova, N. Spaldin, A. Bhattacharya, and P. Ryan, Phys. Rev. B **82**, 014110 (2010).
[18] C. J. M. Daumont, S. Farokhipoor, A. Ferri, J. C. Wojdeł, J. Íñiguez, B. J. Kooi, and B. Noheda, Phys. Rev. B **81**, 144115 (2010).
[19] R. J. Zeches *et al.*, Science **326**, 977 (2009).
[20] C. Merckling, M. El-Kazzi, G. Delhaye, V. Favre-Nicolin, Y. Robach, M. Gendry, G. Grenet, G. Saint-Girons, and G. Hollinger, J. Cryst. Growth **306**, 47 (2007).
[21] N. Reyren *et al.*, Science **317**, 1196 (2007).
[22] M. Huijben, A. Brinkman, G. Koster, G. Rijnders, H. Hilgenkamp, and D. H. A. Blank, Adv. Mater. **21**, 1665 (2009).
[23] R. D. King-Smith and D. Vanderbilt, Phys. Rev. B **47**, 1651 (1993).
[24] D. Vanderbilt and R. D. King-Smith, Phys. Rev. B **48**, 4442 (1993).
[25] S. Denev *et al.*, Phys. Rev. Lett. **100**, 257601 (2008).